Pis'ma v ZhETF, vol. 103, iss. 10, pp. 697 – 701 © 2016 May 25

The decays $\tau \to (\eta, \eta')K^-\nu_\tau$ in the extended Nambu–Jona-Lasinio model

M. K. Volkov[1)], *A. A. Pivovarov*

Bogoliubov Laboratory of Theoretical Physics, JINR, 141980 Dubna, Russia

Submitted 30 March 2016

The decays $\tau \to (\eta, \eta')K^-\nu_\tau$ are described in the framework of the extended Nambu–Jona-Lasinio model. Both full and differential widths of these decays are calculated. The vector and scalar channels are considered. In the vector channel, the subprocesses with the intermediate $K^*(892)$ and $K^*(1410)$ mesons play the main role. In the scalar channel, the subprocesses with the intermediate $K_0^*(800)$ and $K_0^*(1430)$ mesons are taken into account. The scalar channel gives an insignificant contribution to the full width of the decay $\tau \to \eta K^-\nu_\tau$. The obtained results are in satisfactory agreement with the experimental data. The prediction for the width of the process $\tau \to \eta' K^-\nu_\tau$ is made.

DOI: 10.7868/S0370274X16100015

1. Introduction. The τ-decays are a good laboratory for research of strong interactions of mesons at low energies. Since the perturbation theory of quantum chromodynamics is not applicable in this energy region (energy less than $m_\tau = 1.777\,\text{GeV}$), one has to use different phenomenological models. These models are generally based on the vector dominance methods and on the chiral symmetry of strong interactions [1–10]. However, most of these models include a number of fitting parameters for a correct description of experimental data.

The Nambu–Jona-Lasinio (NJL) model [11–20] and its new version — the extended NJL model [20–24] – has a special place among them. These models allow one to avoid introduction of additional arbitrary parameters in the description of the hadron processes at low energies. The extended NJL model is especially useful for research of the τ-lepton decays. In the case of $U(3) \times U(3)$ chiral symmetry, this model allows describing meson nonets in both ground and first radially excited states. At the same time, due to the energy restrictions caused by the τ-lepton mass, intermediate mesons in these states play the main role in some τ-lepton decays. That is why, the use of the extended NJL model allowed a successful description of a series of τ-decays, specifically $\tau \to (\pi, \pi(1300))\nu_\tau$ [25], $\tau \to (\eta, \eta')\pi\nu_\tau$ [26], $\tau \to \pi\omega\nu_\tau$ [27], $\tau \to (\eta, \eta')2\pi$ [28], $\tau \to (\rho(770), \rho(1450))\nu_\tau$, $\tau \to (K^*(892), K^*(1410))\nu_\tau$ [29], $\tau \to K^-\pi^0\nu_\tau$ [30].

In the present work these advantages of the extended NJL model are illustrated by the calculation of the width of the decay $\tau \to \eta K^-\nu_\tau$. Recently, this process has been actively investigated from both experimental [31, 32] and theoretical point of view. One of the most interesting theoretical works on this theme is [8]. In that paper the width of the decay $\tau \to \eta K^-\nu_\tau$ was calculated in the framework of Chiral Perturbation Theory extended by including resonances as active fields, and the prediction of the width of $\tau \to \eta' K^-\nu_\tau$ was made. In that work it is asserted that the use of the Breit–Wigner parametrization does not give satisfactory results in the description of these processes. At the same time, two other methods based on the exponential resummation and dispersive representation provide good fits.

In our work it is shown that in the framework of the extended NJL model the use of the Breit–Wigner relation in the standard form for description of the intermediate states leads to satisfactory results. This statement is confirmed by other calculations pointed above. We also make prediction of the width of the decay $\tau \to \eta' K^-\nu_\tau$, which agrees with the prediction in [8].

2. The Lagrangian of the extended NJL model for the mesons $K^\pm, \eta, \eta', K^{*\pm}, K_0^{*\pm}$ and their first radially excited states. In the extended NJL model, the quark-meson interaction Lagrangian for the pseudoscalar $K^\pm, \eta, \eta'$, scalar $K_0^{*\pm}$, vector $K^{*\pm}$ mesons and their first radially excited states takes the form:

$$\Delta L_{\text{int}} = \bar{q}\left[i\gamma^5 \sum_{j=\pm} \lambda_j (a_K K^j + b_K \hat{K}^j) + \right.$$

$$\left. + \sum_{j=\pm} \lambda_j (a_{K_0^*} K_0^{*j} + b_{K_0^*} \hat{K}_0^{*j}) + \right.$$

[1)] e-mail: volkov@theor.jinr.ru

$$+\frac{1}{2}\gamma^\mu\sum_{j=\pm}\lambda_j(a_{K^*}K^{*j}_\mu+b_{K^*}\hat{K}^{*j}_\mu)+$$

$$+i\gamma^5\sum_{j=u,s}\lambda_j\sum_{\tilde{\eta}=\eta,\eta',\hat{\eta},\hat{\eta}'}A^j_{\tilde{\eta}}\tilde{\eta}\Bigg]q, \qquad (1)$$

where q and $\bar{q}$ are the u-, d-, and s-constituent quark fields with masses $m_u=m_d=280\,\text{MeV}$, $m_s=420\,\text{MeV}$ [24, 33], η, η', $K^\pm$, $K_0^{*\pm}$ and $K^{*\pm}$ are the pseudoscalar, scalar, and vector mesons; the excited states are marked with hat,

$$a_a=\frac{1}{\sin(2\theta^0_a)}\left[g_a\sin(\theta_a+\theta^0_a)+g^{'}_a f_a(\mathbf{k}^2)\sin(\theta_a-\theta^0_a)\right],$$

$$b_a=\frac{-1}{\sin(2\theta^0_a)}\left[g_a\cos(\theta_a+\theta^0_a)+g^{'}_a f_a(\mathbf{k}^2)\cos(\theta_a-\theta^0_a)\right],$$

$$A^j_{\tilde{\eta}}=g^j_1b^j_{\tilde{\eta}1}+g^j_2f_j(\mathbf{k}^2)b^j_{\tilde{\eta}2}, \qquad (2)$$

$f\left(\mathbf{k}^2\right)=1+d\mathbf{k}^2$ is the form factor for description of the first radially excited states [21, 22], d is the slope parameter, θ_a and θ^0_a are the mixing angles for the strange mesons in the ground and excited states,

$$d_{uu}=-1.784\text{GeV}^{-2},\quad d_{us}=-1.761\text{GeV}^{-2},$$
$$d_{ss}=-1.737\text{GeV}^{-2},$$
$$\theta_K=58.11^\circ,\quad \theta_{K^*_0}=74^\circ,\quad \theta_{K^*}=84.74^\circ,$$
$$\theta^0_K=55.52^\circ,\quad \theta^0_{K^*_0}=60^\circ,\quad \theta^0_{K^*}=59.56^\circ. \qquad (3)$$

The insertion of the pseudoscalar isoscalar fields requires consideration of the mixing of the four different states: $\eta,\eta'(958),\eta(1295),\eta(1475)$, which are marked as $\eta,\eta',\hat{\eta},\hat{\eta}'$. The last two ones are considered as the first radially excited states of the η and η' mesons; $b^j_{\tilde{\eta}1}$ and $b^j_{\tilde{\eta}2}$ are the mixing coefficients shown in Table 1 [24].

Table 1. The mixing coefficients for the η-mesons

	η	$\hat{\eta}$	η'	$\hat{\eta}'$
$b^u_{\tilde{\eta}1}$	0.71	0.62	−0.32	0.56
$b^u_{\tilde{\eta}2}$	0.11	−0.87	-0.48	−0.54
$b^s_{\tilde{\eta}1}$	0.62	0.19	0.56	−0.67
$b^s_{\tilde{\eta}2}$	0.06	−0.66	0.30	0.82

These coefficients were successfully applied for description of a series of processes with the η-mesons [24, 28, 34].

The matrices

$$\lambda_+=\frac{\lambda_4+i\lambda_5}{\sqrt{2}},\qquad \lambda_u=\frac{\sqrt{2}\lambda_0+\lambda_8}{\sqrt{3}},$$
$$\lambda_-=\frac{\lambda_4-i\lambda_5}{\sqrt{2}},\qquad \lambda_s=\frac{-\lambda_0+\sqrt{2}\lambda_8}{\sqrt{3}},$$
$$\lambda_0=\sqrt{\tfrac{2}{3}}\hat{\mathbf{1}}, \qquad (4)$$

λ_4, λ_5 and λ_8 are the Gell-Mann matrices.

The coupling constants:

$$g_K=\left(\frac{4}{Z_K}I_2(m_u,m_s)\right)^{-1/2}\approx 3.77,$$
$$g^{'}_K=\left(4I_2^{f^2_{us}}(m_u,m_s)\right)^{-1/2}\approx 4.69,$$
$$g_{K^*_0}=(4I_2(m_u,m_s))^{-1/2}\approx 2.78,$$
$$g^{'}_{K^*_0}=\left(4I_2^{f^2_{us}}(m_u,m_s)\right)^{-1/2}\approx 4.69,$$
$$g_{K^*}=\left(\frac{2}{3}I_2(m_u,m_s)\right)^{-1/2}\approx 6.81,$$
$$g^{'}_{K^*}=\left(\frac{2}{3}I_2^{f^2_{us}}(m_u,m_s)\right)^{1/2}\approx 11.49,$$
$$g^u_1=\left(\frac{4}{Z_\pi}I_2(m_u,m_u)\right)^{-1/2}\approx 3.02,$$
$$g^u_2=\left(4I_2^{f^2_{uu}}(m_u,m_u)\right)^{-1/2}\approx 4.03,$$
$$g^s_1=\left(\frac{4}{Z_s}I_2(m_s,m_s)\right)^{-1/2}\approx 4.41,$$
$$g^s_2=\left(4I_2^{f^2_{ss}}(m_s,m_s)\right)^{-1/2}\approx 5.39, \qquad (5)$$

where

$$Z_\pi=\left(1-6\frac{m^2_u}{M^2_{a_1}}\right)^{-1}\approx 1.45,$$
$$Z_s=\left(1-6\frac{m^2_s}{M^2_{f_1}}\right)^{-1}\approx 2.09,$$
$$Z_K=\left(1-\frac{3}{2}\frac{(m_u+m_s)^2}{M^2_{K_1}}\right)^{-1}\approx 1.83, \qquad (6)$$

Z_π is the factor corresponding to the $\eta-a_1$ transitions, Z_K is the factor corresponding to the $K-K_1$ transitions, Z_s is the factor corresponding to the $\eta-f_1$ transitions, $M_{a_1}=1230$ MeV, $M_{K_1}=1272$ MeV, $M_{f_1}=1426$ MeV [35] are the masses of the axial-vector a_1, K_1 and f_1 mesons, and the integral I_2 has the following form:

$$I_2^{f^n}(m_1,m_2)=$$
$$=-i\frac{N_c}{(2\pi)^4}\int\frac{f^n(\mathbf{k^2})}{(m^2_1-k^2)(m^2_2-k^2)}\theta(\Lambda^2_3-\mathbf{k}^2)d^4k, \qquad (7)$$

$\Lambda_3=1.03\,\text{GeV}$ is the cut-off parameter [14].

All these parameters were calculated earlier and are standard for the extended NJL model [22, 24].

3. The amplitude of the decay $\tau\to\eta K^-\nu_\tau$ in the extended NJL model. The diagrams of the process $\tau\to\eta K^-\nu_\tau$ are shown in Figs. 1 and 2.

3.1. The vector channel. The amplitude of the process $\tau\to\eta K^-\nu_\tau$ for the vector channel takes the form:

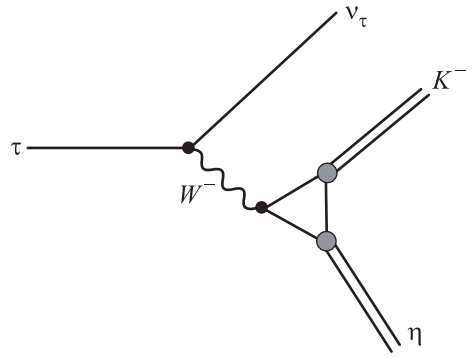

Fig. 1. The decay $\tau \to \eta K^-\nu_\tau$ with the intermediate W-boson (contact diagram)

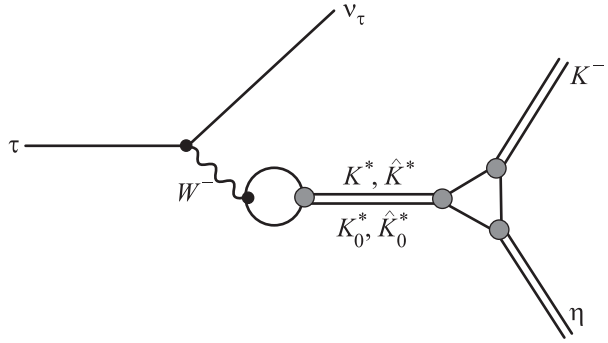

Fig. 2. The decay $\tau \to \eta K^-\nu_\tau$ with the intermediate vector $K^*(892)$, $K^*(1410)$ and scalar $K_0^*(800)$, $K_0^*(1430)$ mesons

$$T_V = -2iG_F|V_{us}|l^\mu\Big\{C_1 g_{\mu\nu} + \frac{C_2C_3}{g_{K^*}} \times$$
$$\times \frac{g_{\mu\nu}q^2 - q_\mu q_\nu - g_{\mu\nu}\frac{3}{2}(m_s-m_u)^2}{M^2_{K^*} - q^2 - i\sqrt{q^2}\Gamma_{K^*}} + \frac{C_2^{'}C_3^{'}}{g_{K^*}} \times$$
$$\times \frac{g_{\mu\nu}q^2 - q_\mu q_\nu - g_{\mu\nu}\frac{3}{2}(m_s-m_u)^2}{M^2_{\hat{K}^*} - q^2 - i\sqrt{q^2}\Gamma_{\hat{K}^*}}\Big\}(p_K - p_\eta)^\nu, \quad (8)$$

where $G_F = 1.16637 \cdot 10^{-11}\,\text{MeV}^{-2}$ is the Fermi constant, $V_{us} = 0.2252$ is the element of the Cabbibo–Kobayashi–Maskawa matrix, $l^\mu = \bar{\nu}_\tau\gamma^\mu\tau$ is the lepton current, $q = p_K + p_\eta$, $M_{K^*} = 896\,\text{MeV}$, $M_{\hat{K}^*} = 1414\,\text{MeV}$, $\Gamma_{K^*} = 46\,\text{MeV}$, $\Gamma_{\hat{K}^*} = 232\,\text{MeV}$ are the masses and the full widths of the vector mesons [35].

The first term corresponds to the diagram with the intermediate W-boson, the second and the third terms correspond to the diagrams with the intermediate vector mesons $K^*(892)$ and $K^*(1410)$. The part

$$\frac{C_2(C_2^{'})}{g_{K^*}}\left[g_{\mu\nu}q^2 - q_\mu q_\nu - g_{\mu\nu}\frac{3}{2}(m_s-m_u)^2\right]$$

is obtained from the quark loop in the transition of the W-boson into the intermediate vector meson. The part $C_1(C_3, C_3^{'})(p_K - p_\eta)^\nu$ comes from the quark triangle. The numerical coefficients are

$$C_1 = I^{a_K A_\eta^u} + \sqrt{2}I^{a_K A_\eta^s},$$

$$C_2 = \frac{1}{\sin(2\theta^0_{K^*})}[\sin(\theta_{K^*} + \theta^0_{K^*}) + R_V\sin(\theta_{K^*} - \theta^0_{K^*})],$$

$$C_2^{'} = \frac{-1}{\sin(2\theta^0_{K^*})}[\cos(\theta_{K^*} + \theta^0_{K^*}) + R_V\cos(\theta_{K^*} - \theta^0_{K^*})],$$

$$C_3 = I^{a_K a_{K^*} A_\eta^u} + \sqrt{2}I^{a_K a_{K^*} A_\eta^s},$$
$$C_3^{'} = I^{a_K b_{K^*} A_\eta^u} + \sqrt{2}I^{a_K b_{K^*} A_\eta^s}, \quad (9)$$

where

$$R_V = \frac{I_2^{f_{us}}(m_u, m_s)}{\sqrt{I_2(m_u, m_s)I_2^{f^2_{us}}(m_u, m_s)}},$$

$$I^{abc} = -i\frac{N_c}{(2\pi)^4}\int\frac{a(\mathbf{k}^2)b(\mathbf{k}^2)c(\mathbf{k}^2)}{(m_s^2 - k^2)(m_u^2 - k^2)}\theta(\Lambda_3^2 - \mathbf{k}^2)d^4k,$$

and where $a(\mathbf{k}^2)$, $b(\mathbf{k}^2)$ and $c(\mathbf{k}^2)$ are the coefficients from the Lagrangian defined in (2).

3.2. The scalar channel. The amplitude of the process $\tau \to \eta K^-\nu_\tau$ for the scalar channel takes the form:

$$T_S = -4iG_F|V_{us}|l^\mu \times$$
$$\times\left\{\frac{C_4C_5}{g_{K_0^*}}\cdot\frac{m_s - m_u}{M^2_{K_0^*} - q^2 - i\sqrt{q^2}\Gamma_{K_0^*}} + \right.$$
$$\left. + \frac{C_4^{'}C_5^{'}}{g_{K_0^*}}\cdot\frac{m_s - m_u}{M^2_{\hat{K}_0^*} - q^2 - i\sqrt{q^2}\Gamma_{\hat{K}_0^*}}\right\}q_\mu, \quad (10)$$

where $M_{K_0^*} = 682\,\text{MeV}$, $M_{\hat{K}_0^*} = 1425\,\text{MeV}$, $\Gamma_{K_0^*} = 547\,\text{MeV}$ and $\Gamma_{\hat{K}_0^*} = 270\,\text{MeV}$ are the masses and full widths of the scalar mesons [35].

The part $\frac{C_4(C_4^{'})}{g_{K_0^*}}(m_s - m_u)$ is obtained from the quark loop in the transition of the W-boson into the intermediate scalar meson. The part $C_5(C_5^{'})q_\mu$ comes from the quark triangle. The numerical coefficients are

$$C_4 = \frac{1}{\sin\left(2\theta^0_{K_0^*}\right)} \times$$
$$\times\left[\sin\left(\theta_{K_0^*} + \theta^0_{K_0^*}\right) + R_V\sin\left(\theta_{K_0^*} - \theta^0_{K_0^*}\right)\right],$$
$$C_4^{'} = \frac{-1}{\sin\left(2\theta^0_{K_0^*}\right)} \times$$
$$\times\left[\cos\left(\theta_{K_0^*} + \theta^0_{K_0^*}\right) + R_V\cos\left(\theta_{K_0^*} - \theta^0_{K_0^*}\right)\right],$$
$$C_5 = m_s I^{a_K a_{K_0^*} A_\eta^u} - \sqrt{2}m_u I^{a_K a_{K_0^*} A_\eta^s},$$
$$C_5^{'} = m_s I^{a_K b_{K_0^*} A_\eta^u} - \sqrt{2}m_u I^{a_K b_{K_0^*} A_\eta^s}. \quad (11)$$

4. Numerical estimations. The contribution of the diagrams with the vector channel to the branching of the process $\tau \to \eta K^- \nu_\tau$ is

$$Br(\tau \to \eta K^- \nu_\tau)_V = 1.46 \cdot 10^{-4}. \quad (12)$$

The contribution of the scalar channel is

$$Br(\tau \to \eta K^- \nu_\tau)_S = 0.28 \cdot 10^{-7}. \quad (13)$$

The calculated branching of the whole process is

$$Br(\tau \to \eta K^- \nu_\tau)_{\rm tot} = 1.45 \cdot 10^{-4}. \quad (14)$$

The experimental values of this branching are

$$Br(\tau \to \eta K^- \nu_\tau)_{\rm exp} = (1.58 \pm 0.14) \cdot 10^{-4}, \ [31]$$
$$Br(\tau \to \eta K^- \nu_\tau)_{\rm exp} = (1.42 \pm 0.18) \cdot 10^{-4}, \ [32]$$
$$Br(\tau \to \eta K^- \nu_\tau)_{\rm exp} = (1.52 \pm 0.08) \cdot 10^{-4}. \ [35] \quad (15)$$

In conclusion, let us note that we have not taken into account the dependence of the width of $K^*(892)$ on the momentum. If we assume that it grows linearly in $\sqrt{q^2}$, then in the considered energy region one can put $\Gamma_{K^*} \approx 70\,$MeV. Then the whole branching is

$$Br(\tau \to \eta K^- \nu_\tau) = 1.54 \cdot 10^{-4}. \quad (16)$$

The comparison of the calculated and experimental differential widths is shown in Fig. 3. The solid line

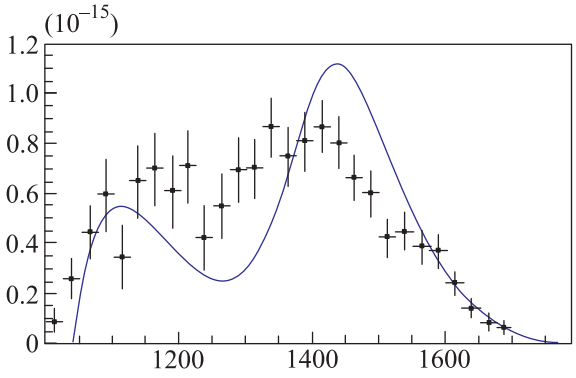

Fig. 3. (Color online)Differential width of the decay $\tau \to \eta K^- \nu_\tau$

corresponds to our theoretical differential width. The points correspond to the experimental values [31].

The prediction for the branching of the process $\tau \to \eta' K^- \nu_\tau$ is obtained similarly. The contribution of the vector channel is

$$Br(\tau \to \eta' K^- \nu_\tau)_V = 1.69 \cdot 10^{-6}. \quad (17)$$

The contribution of the scalar channel is

$$Br(\tau \to \eta' K^- \nu_\tau)_S = 0.77 \cdot 10^{-7}. \quad (18)$$

The branching of the whole process is

$$Br(\tau \to \eta' K^- \nu_\tau)_{\rm tot} = 1.25 \cdot 10^{-6}. \quad (19)$$

The experimental value is [35]

$$Br(\tau \to \eta' K^- \nu_\tau)_{\rm exp} < 2.4 \cdot 10^{-6}. \quad (20)$$

The prediction of the differential width of the process $\tau \to \eta' K^- \nu_\tau$ is shown in Fig. 4.

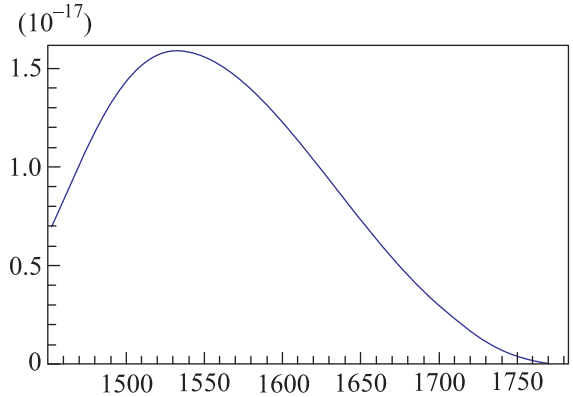

Fig. 4. (Color online) Differential width of the decay $\tau \to \eta' K^- \nu_\tau$

5. Conclusion. The calculations carried out in the framework of the extended NJL model show that the main contribution to the width of the decay $\tau \to \eta K^- \nu_\tau$ is given by the vector channel. The subprocesses with the intermediate $K^*(892)$ and $K^*(1410)$ mesons play the principal role. The channel with the intermediate scalar mesons gives a negligible contribution. The obtained results are in satisfactory agreement with the experimental data. The prediction for the width of the process $\tau \to \eta' K^- \nu_\tau$ was made.

The right shift of the main peak of our theoretical differential width of the process $\tau \to \eta K^- \nu_\tau$ may be explained by a wrong choice of the mass of $K^*(1410)$, which is not measured precisely enough [36, 37]. The experimentally observed small bump of the differential width in the region of 1600 MeV may be explained by the existence of the second radially excited state $K^*(1680)$, which was not taken into account here.

We are grateful to A.B. Arbuzov and O.V. Teryaev for useful discussions; this work is supported by the grant of RFBR # 14-01-00647.

1. M. Finkemeier and E. Mirkes, Z. Phys. C **72**, 619 (1996).
2. B. A. Li, Phys. Rev. D **55**, 1436 (1997).
3. S. Fajfer and J. Zupan, Int. J. Mod. Phys. A **14**, 4161 (1999).

4. A. A. Andrianov and V. A. Andrianov, Int. J. Mod. Phys. A **20**, 1850 (2005).
5. S. Nussinov and A. Soffer, Phys. Rev. D **80**, 033010 (2009).
6. N. Paver and Riazuddin, Phys. Rev. D **84**, 017302 (2011).
7. D. G. Dumm and P. Roig, Phys. Rev. D **86**, 076009 (2012).
8. R. Escribano, S. Gonzalez-Solis, and P. Roig, JHEP **1310**, 039 (2013).
9. R. Escribano, S. Gonzalez-Solis, M. Jamin, and P. Roig, JHEP **1409**, 042 (2014).
10. X.-W. Kang, B. Kubis, C. Hanhart, and U.-G. Meissner, Phys. Rev. D **89**, 053015 (2014).
11. T. Eguchi, Phys. Rev. D **14**, 2755 (1976).
12. D. Ebert and M. K. Volkov, Z. Phys. C **16**, 205 (1983).
13. M. K. Volkov, Ann. Phys. **157**, 282 (1984).
14. M. K. Volkov, Sov. J. Part. Nucl. **17**, 186 (1986) [Fiz. Elem. Chast. Atom. Yadra **17**, 433 (1986)].
15. D. Ebert and H. Reinhardt, Nucl. Phys. B **271**, 188 (1986).
16. U. Vogl and W. Weise, Prog. Part. Nucl. Phys. **27**, 195 (1991).
17. S. P. Klevansky, Rev. Mod. Phys. **64** 649 (1992).
18. M. K. Volkov, Phys. Part. Nucl. **24**, 35 (1993).
19. D. Ebert, H. Reinhardt, and M. K. Volkov, Prog. Part. Nucl. Phys **33**, 1 (1994).
20. M. K. Volkov and A. E. Radzhabov, Phys. Usp. **49**, 551 (2006).
21. M. K. Volkov and C. Weiss, Phys. Rev. D **56**, 221 (1997).
22. M. K. Volkov, Phys. Atom. Nucl. **60**, 1920 (1997) [Yad. Fiz. **60**, 2094 (1997)].
23. M. K. Volkov, D. Ebert, and M. Nagy, Int. J. Mod. Phys. A **13**, 5443 (1998).
24. M. K. Volkov and V. L. Yudichev, Phys. Part. Nucl. **31**, 282 (2000) [Fiz. Elem. Chast. At. Yadra **31**, 576 (2000)].
25. A. I. Ahmadov and M. K. Volkov, Phys. Part. Nucl. Lett. **12**, 744 (2015).
26. M. K. Volkov and D. G. Kostunin, Phys. Rev. D **86**, 013005 (2012).
27. M. K. Volkov, A. B. Arbuzov, and D. G. Kostunin, Phys. Rev. D **86**, 057301 (2012).
28. M. K. Volkov, A. B. Arbuzov, and D. G. Kostunin, Phys. Rev. C **89**, 015202 (2014).
29. A. I. Ahmadov, Yu. L. Kalinovsky, and M. K. Volkov, Int. J. Mod. Phys. A **30**, 1550161 (2015).
30. M. K. Volkov and A. A. Pivovarov, Mod. Phys. Lett. A **31** 1650043 (2016); arXiv:1511.08332 [hep-ph].
31. Belle Collaboration (K. Inami (Nagoya U.) et al.), Phys. Lett. B **672**, 209 (2009).
32. BaBar Collaboration (P. del Amo Sanchez (Annecy, LAPP) et al.), Phys. Rev. D **83**, 032002 (2011).
33. M. K. Volkov and V. L. Yudichev, Eur. Phys. J. A **10**, 109 (2001).
34. A. I. Ahmadov, D. G. Kostunin, and M. K. Volkov, Phys. Rev. C **87**, 045203 (2013).
35. K. A. Olive et al. (Particle Data Group), Chin. Phys. C **38**, 090001 (2014); 2015 (update).
36. D. Aston, N. Awaji, T. Bienz et al. (Collaboration), Nucl. Phys. B **296**, 493 (1988).
37. D. Aston, N. Awaji, J. D'Amore et al. (Collaboration), Nucl. Phys. B **292**, 693 (1987).